Ephrin-B3 Ligand Promotes Glioma Invasion through Activation of Rac1

Mitsutoshi Nakada, Kelsey L. Drake, Satoko Nakada, Jared A. Niska, and Michael E. Berens

The Translational Genomics Research Institute, Phoenix, Arizona

Abstract

Eph receptor tyrosine kinases are involved in nervous system development. Eph ligands, termed ephrins, are transmembrane proteins that bind to Eph receptors, the mutual activation of which causes repulsive effects in reciprocally contacting cells. Previously, we showed that overexpression of EphB2 in glioma cells increases cell invasion. Here, expression profiles of ephrin-B family members were determined in four glioma cell lines and in invading glioblastoma cells collected by laser capture microdissection. Ephrin-B3 mRNA was up-regulated in migrating cells of four of four glioma cell lines (1.3- to 1.7-fold) and in invading tumor cells of eight of eight biopsy specimens (1.2- to 10.0-fold). Forced expression of ephrin-B3 in low expressor cell lines (U87, T98G) stimulated cell migration and invasion *in vitro* and *ex vivo*, concomitant with tyrosine phosphorylation of ephrin-B3. In high expressor cell lines (U251, SNB19), ephrin-B3 colocalized with Rac1 to lamellipodia of motile wild-type cells. Cells transfected with ephrin-B3 small interfering RNA (siRNA) showed significant morphologic change and decreased invasion *in vitro* and *ex vivo*. Depletion of endogenous ephrin-B3 expression abrogated the increase of migration and invasion induced by EphB2/Fc, indicating increased invasion is dependent on ephrin-B3 activation. Furthermore, using a Rac1-GTP pull-down assay, we showed that ephrin-B3 is associated with Rac1 activation. Reduction of Rac1 by siRNA negated the increased invasion by addition of EphB2/Fc. In human glioma specimens, ephrin-B3 expression and phosphorylation correlated with increasing tumor grade. Immunohistochemistry revealed robust staining for phosphorylated ephrin-B and ephrin-B3 in invading glioblastoma cells. These data show that ephrin-B3 expression and signaling through Rac1 are critically important to glioma invasion. (Cancer Res 2006; 66(17): 8492-500)

Introduction

Eph proteins form the largest family of receptor tyrosine kinases in the human genome, with 16 Eph receptors and 9 ephrin ligands (1). Eph receptors and their ligands are involved in various aspects of the development of the nervous system, including morphogenesis, vascular formation, and cell migration (2–7). There are two classes of Eph receptors: EphA and EphB. Upon ligand binding, Eph receptors dimerize and become phosphorylated (7). Ligands for Eph receptors are classified as ephrin-A or ephrin-B, based on the type of Eph with which they interact. A-type ephrins are anchored to the plasma membrane via glycosylphosphotidylinositol linkages, whereas B-type ephrins have a transmembrane domain and an intracellular domain, which includes sites for tyrosine phosphorylation and a docking site for proteins with a PDZ domain. These sites give ephrin-B ligands at least two ways to engage in protein-protein interactions (3). As a result, when cells expressing ephrin-B contact cells expressing Eph kinases, bidirectional signaling can occur (8). Considerable efforts have been made in recent years to elucidate the forward signaling by EphB (9–11). However, the function of reverse signaling by ephrin-B remains largely unknown.

Eph family members have been implicated in cellular transformation, metastasis, and angiogenesis (12, 13), and their up-regulation has been described in a range of human tumors and cell lines (14–20). We recently showed that EphB2 plays a role in the invasive behavior of glioma (21). In contrast, little is currently known about the role of the ephrin-B ligand family members in the malignant phenotype of cancer, although our microarray results identified the expression of ephrin-B3 in invading glioma cells *in situ* (22).

We recently revealed that R-Ras, which is a member of the intracellular small GTPase family, mediates EphB2 signaling in invading glioma cells (23). The ephrin-B1 signaling cascade, which participates in the regulation of neurite outgrowth, involves activation of Rac1, which is also a small GTPase (24). Thus, coincident to Eph-ephrin transactivation on adjoining cells, signaling molecules involved in cytoskeletal organization are recruited to both Ephs and ephrins, supporting the concept that cytoskeletal plasticity is driven by direct communication of Eph/ephrins with the intracellular machinery (6). Moreover, Rac1 is an important regulator of the motility of glioma cells through the organization of the actin cytoskeleton (25, 26). These findings prompt examination of the effect of specific ephrin-B ligands on glioma invasion, and the function of specific small GTPases as possible mediators of activated ephrin-B intracellular signaling.

In this study, we analyzed the role of the ephrin-B ligand family in invading glioma cells. Expression of the ephrin-B family was examined in migrating glioma cells *in vitro* and invading glioma cells *in vivo*. Forced expression of ephrin-B3 in human glioma cells induces invasion both *in vitro* and *ex vivo*. Small interfering RNA (siRNA) that knocked out ephrin-B3 inhibits glioma invasion *in vitro* and *ex vivo*. Furthermore, we showed that phosphorylation of ephrin-B3 induces activation of Rac1, whereas depletion of ephrin-B3 deactivates Rac1. In human glioblastoma specimens, ephrin-B3 is overexpressed and phosphorylated. These results suggest that ephrin-B3 signaling through Rac1 plays an important role in the invasive behavior of glioma.

Materials and Methods

Cell culture. Human astrocytoma cell lines U87, T98G, U251 and SNB19 (American Type Culture Collection, Manassas, VA), and SF767 (27) were maintained in DMEM supplemented with 10% fetal bovine serum at 37°C.

Note: Supplementary data for this article are available at Cancer Research Online (http://cancerres.aacrjournals.org/).

Requests for reprints: Michael E. Berens, The Translational Genomics Research Institute, 445 North Fifth Street, Phoenix, AZ 85004. Phone: 602-343-8760; Fax: 602-343-8844; E-mail: mberens@tgen.org.

doi:10.1158/0008-5472.CAN-05-4211

Antibodies and reagents. Antiphosphotyrosine and anti-phospho-ephrin-B monoclonal antibodies were purchased from Cell Signaling Technology (Beverly, MA). Anti-ephrin-B3 antibody for immunocytochemistry and immunohistochemistry, and EphB2/Fc chimera, were obtained from R&D Systems (Minneapolis, MN). Anti-ephrin-B3 polyclonal antibody for immunoprecipitation and immunoblot analysis was purchased from Invitrogen (Carlsbad, CA). An α-tubulin monoclonal antibody was obtained from Oncogene Research (Boston, MA). Anti-Rac1 monoclonal antibody was purchased from BD Biosciences PharMingen (San Diego, CA). Control Fc fragment of mouse IgG was from Sigma (St. Louis, MO).

Migration assay. Migration assays were done using the microliter-scale radial monolayer migration assay as described previously (28). To assess the ephrin-B expression level in different cell conditions, cells actively migrating at the rim and migration-restricted cells at the core were mechanically collected as separate populations after 24 hours of cell motility. RNA was isolated from the two cell populations and quantitative real-time-PCR (QRT-PCR) was done.

To investigate the influence of ephrin-B3 phosphorylation on glioma cell motility, cells transfected with vector or siRNA were seeded in the migration assay format and allowed to adhere. The medium was then exchanged for serum-free medium containing 1 μg/mL of recombinant EphB2/Fc chimera or control Fc and the migration rate was evaluated for 24 hours.

Clinical samples and histology. Following an institutional review board–approved protocol, fresh human brain tumor tissues were obtained from 41 patients who underwent therapeutic removal of astrocytic brain tumors. Nonneoplastic control brain tissues were identified from the margins of the tumors. Histologic diagnosis was made by standard light microscopic evaluation of the sections stained with H&E. The classification of human brain tumors used in this study is based on the revised WHO criteria for tumors of the central nervous system (29). The 41 astrocytic tumors consisted of 7 low-grade astrocytomas, 4 anaplastic astrocytomas, and 30 glioblastomas. All of the tumor tissues were obtained at primary resection, and none of the patients had been subjected to chemotherapy or radiation therapy before resection.

Laser capture microdissection. Cryopreserved glioblastoma specimens from eight patients were cut in serial 6 to 8 μm sections and mounted on uncoated slides treated with diethyl pyrocarbonate. Laser capture microdissection was then done with a PixCell II Microscope (Arcturus Engineering, Inc., Mountain View, CA). Three thousand individual neoplastic cells were collected from invasive rim and from tumor core for QRT-PCR analysis as described previously (21, 30).

QRT-PCR. QRT-PCR was carried out in a LightCycler (Roche Diagnostics, Indianapolis, IN) as described previously (30). PCR was done with the following primers: ephrin-B3 (NM_001406): sense, 5′-ATGTGCTCTCCC-GAGTAACC-3′; antisense, 5′-GGAGGAAACTGAGGCAACAC-3′ (amplicon size, 223 bp); histone H3.3 (NM_002107): sense, 5′-CCACTGAACTTCT-GATTCGC-3′; antisense, 5′-GCGTGCTAGCTGGATGTCTT-3′ (amplicon size, 215 bp). The nucleotide number and amplicon size for each primer are within parentheses. The LightCycler analysis software was used to analyze the PCR data, as described previously (30).

Expression plasmids and cell transfection. An expression plasmid for ephrin-B3 was constructed as follows: a cDNA fragment encoding ephrin-B3 was PCR-amplified using human embryonic kidney 293T cDNA as a template; the fragment was then inserted into a pEAK plasmid. Transient transfection was done with U87 and T98G cells using Effectene (Qiagen, Valencia, CA), as recommended by the protocol of the manufacturer. Cells transfected with empty plasmid vector were used as controls.

Immunoprecipitation and immunoblot analysis. Immunoprecipitation and immunoblot analyses were done as described previously (23). Equivalent amounts of protein (300 μg) were precleared, then immunoprecipitated from the lysates. To detect phosphorylation of ephrin-B3, cells were stimulated by EphB2/Fc for 10 minutes at 37°C before cell lysate extraction.

Cell invasion assay. Cell invasion assays were done using Boyden chambers consisting of Transwells with precoated Matrigel membrane filter inserts in 24-well tissue culture plates (BD Biosciences Discovery Labware, Bedford, MA) as described previously (31, 32). In certain experiments, EphB2/Fc or control Fc fragment of mouse IgG was applied to the upper chamber.

***Ex vivo* invasion assay on rat brain slices.** The *ex vivo* invasion assay into rat brain slices was carried out as described previously (21, 26). Approximately 1×10^5 glioma cells stably expressing green fluorescence protein (GFP) were gently applied (0.5 μL transfer volume) to the putamen of the brain slice. Imaging of specimens was done at ×10 magnification using a Macro-Fluorescent Imaging System (SZX12-RFL3; Olympus, Tempe, AZ) equipped with a GFP barrier filter (DP50; Olympus) at 12 and 48 hours after seeding the cells. Glioma cell invasion into the rat brain slices was quantitated using a Laser scanning confocal microscope (Zeiss, Thornwood, NY) to observe GFP-labeled cells. The invasion rate was calculated as described previously (21, 33).

Silencing of endogenous Ephrin-B3 with siRNA. Purified, duplexed siRNAs for ephrin-B3, Rac1, and control luciferase were purchased from Qiagen. The two target sequences of human ephrin-B3 (Genbank accession number NM_001406) were (748-766 bp) 5′-CCAGGAGTATAGCCCTAAT-3′ and (786-804 bp) 5′-GCTCGCACCACGATTACTA-3′. The sequences were designed to be unique relative to the sequences of other ephrin members. The target sequence of human Rac1 (AF498964) was (439-459 bp) 5′-AAGGAGATTGGTGCTGTAAAA-3′, as described previously (26, 34). Twenty nanomolar siRNA was transfected into U251 and SNB19 cells cultured in 60-mm-diameter dishes using Lipofectamine 2000 (Invitrogen) as recommended by the protocol of the manufacturer. Transfected cells were cultured for 48 hours before use.

Immunofluorescent microscopy and immunohistochemistry. For immunofluorescence, cells were fixed in 4% paraformaldehyde and then permeabilized. After washing with PBS, cells were blocked with 2% bovine serum albumin and 3% goat serum and incubated with anti-ephrin-B3 antiserum (1:100 dilution) or anti-Rac1 antiserum (1:100 dilution) for 1 hour at 25°C. Negative controls were stained with a 1:50 dilution of preimmunization mouse sera. Cells were incubated for 30 minutes with 1:100 dilution of Cy3-conjugated anti-goat antibody or fluorescein-isothiocyanate-conjugated anti-mouse antibody (The Jackson Laboratory, Bar Harbor, ME). Staining for filamentous actin (F-actin) was done with Texas red–conjugated phalloidin (Invitrogen). Fluorescence was monitored by inverted confocal laser microscopy.

Immunohistochemistry was done using avidin-biotin immunoperoxidase technique as described previously (23). Anti-phospho-ephrin-B and anti-ephrin-B3 antibodies were used at a dilution of 1:100.

Rac1-GTP pull-down assay. The active form of Rac1 was detected using EZ-Detect Rac1 Activation kit (Pierce, Rockford, IL) as recommended by the protocol of the manufacturer. U87 and U251 cells cultured in 10 cm dishes were transfected with ephrin-B3 vector and ephrin-B3 siRNA, respectively. Cells were treated with 1.0 μg/mL EphB2/Fc or control Fc for 10 minutes before collection. GTP-Rac1 was detected using the monoclonal antibody against Rac1 included in the kit.

Statistics. Statistical analyses were done using the χ^2 test, the two-tailed Mann-Whitney U test and two-way ANOVA. $P < 0.05$ was considered significant.

Results

Actively migrating and invading glioma cells have increased expression of ephrin-B3. Because the EphB/ephrin-B system has been described as a factor in glioma cell motility (21), we characterized the expression of various ephrin-B ligands in the migrating and nonmigrating states of four glioma cell lines. To evaluate the expression level of ephrin-B across different cell lines, the expression level of core U87 mRNA was arbitrarily chosen to normalize the data. Only ephrin-B3, among all ligands of the ephrin-B family, was overexpressed in the migrating cells relative to the migration-restricted cells at the core of the assay in all cell lines (1.3- to 1.7-fold; Fig. 1*A*). To investigate the role of ephrin-B in invasion *in vivo*, invading glioblastoma cells and cells at the tumor core were collected by laser capture microdissection from eight

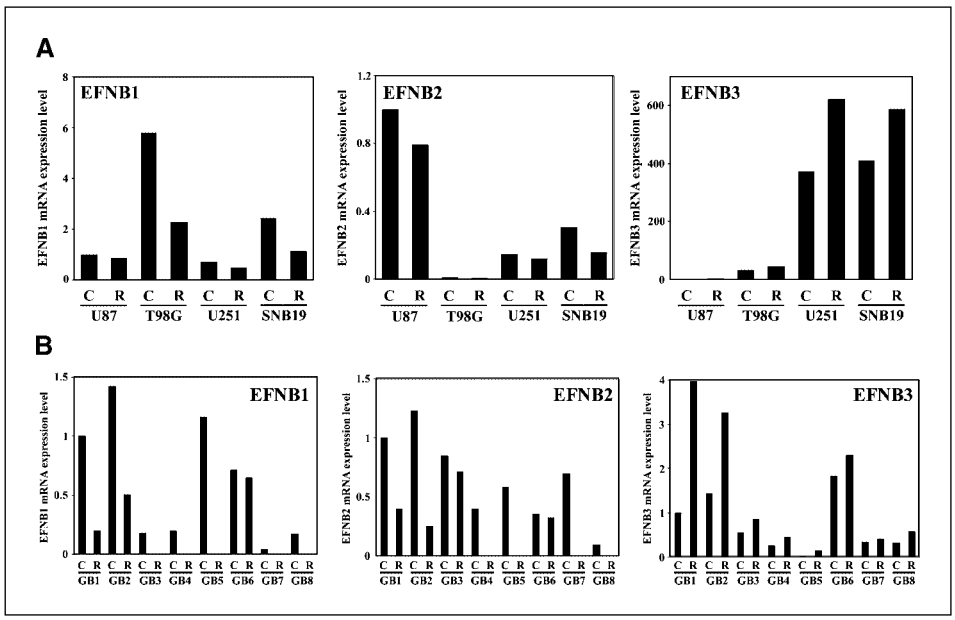

Figure 1. The profile of ephrin-B mRNA expression in glioma cells. *A,* relative mRNA expression levels of ephrin-B family genes (target mRNA/histone H3.3 mRNA ratios) in cells at the core (*C*) and rim (*R*) of the migration assay were analyzed by QRT-PCR. Each mRNA level is expressed as a proportion of the U87 core mRNA level, which was given a value of 1. *B,* tumor core cells (*C*) and invading cells (*R*) in eight glioblastoma cases (*GB1-GB8*) were collected using laser capture microdissection and ephrin-B family gene expression was determined by QRT-PCR. Each mRNA level was expressed as a proportion of the mRNA level of EphB2 in the GB1 core, which was given a value of 1. Results shown in (*A* and *B*) are typical of at least two replicate experiments.

snap-frozen glioblastoma surgical specimens. QRT-PCR was then done on the isolated RNA. Consistent with *in vitro* data, only ephrin-B3 was overexpressed in invading glioblastoma cells (1.2- to 10.0-fold) relative to tumor core cells in eight of eight (100%) biopsy specimens (Fig. 1*B*).

Ephrin-B3 phosphorylation promotes migration and invasion of glioma cells *in vitro* and *ex vivo*. Because ephrin-B3 mRNA levels are elevated during glioma cell migration and invasion, we investigated the activation of ephrin-B3 as a possible stimulant of glioma cell migration and invasion. Ephrin-B3 vector was transfected into U87 and T98G cells, which are low expressors of ephrin-B3 (Fig. 1*A*). Forced expression of the ephrin-B3 ligand was accompanied by phosphorylation of the transfected ligand and was further promoted by addition of recombinant EphB2/Fc chimera in both U87 and T98G (Fig. 2*A*).

Microliter-scale monolayer migration assays revealed that overexpression of ephrin-B3 in U87 and T98G cells induced an increase in migration rate (mean ± SD, 22.90 ± 0.86 μm/h, $P < 0.01$; 13.66 ±

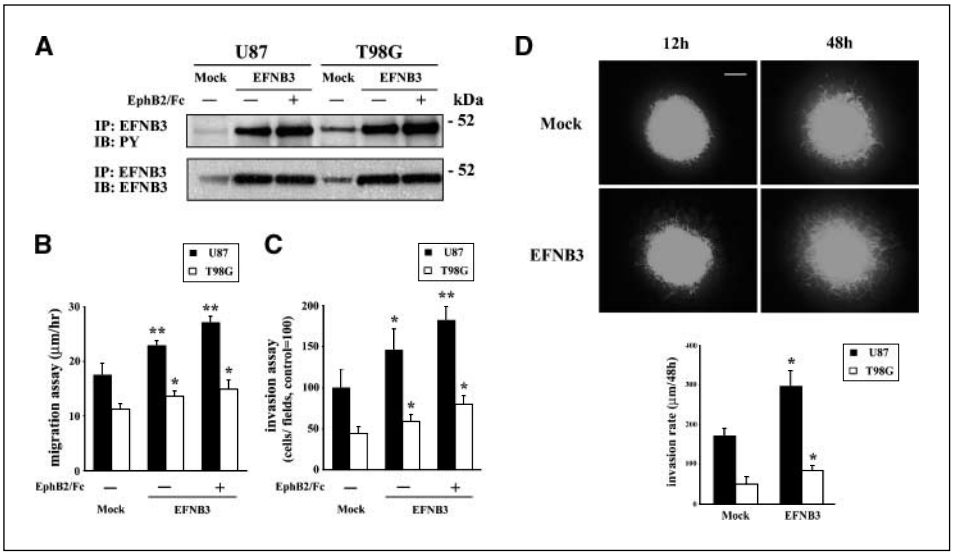

Figure 2. The influence of ephrin-B3 phosphorylation on migration and invasion of U87 and T98G cells. *A,* phosphorylation of ephrin-B3 in transiently transfected U87 and T98G cells. Ephrin-B3 was immunoprecipitated from cells transfected with pEAK (mock) or ephrin-B3 vector and treated with 1.0 μg/mL soluble EphB2/Fc chimera or control Fc for 10 minutes. The immunoprecipitates were probed by immunoblotting as indicated. *B,* cells were plated onto 10-well glass slides precoated with astrocytoma-derived extracellular matrix, and then cultured in serum-free medium in the absence or presence of 1.0 μg/mL soluble EphB2/Fc after the attachment of the cells to the dishes. *Columns,* cell migration assessed over 24 hours; *bars*, SE. *, $P < 0.05$; **, $P < 0.01$ versus mock. *C,* cells were treated as above, then applied to the invasion assay. *Columns,* mean cell counts from at least six fields in each of four experiments; *bars*, SE. *, $P < 0.05$; **, $P < 0.01$ versus mock. *D,* U87 glioma cells stably expressing GFP were transfected with pEAK or ephrin-B3, 2 days before implantation into the bilateral putamen on a rat organotypic brain slice and observed at the indicated times. Bar, 500 μm. *Columns,* invasion rates of cells treated with vectors, calculated from *Z*-axis images collected by confocal laser scanning microscopy; *bars*, SE. *, $P < 0.05$ versus mock. The mean value of invasion rates was obtained from six independent experiments.

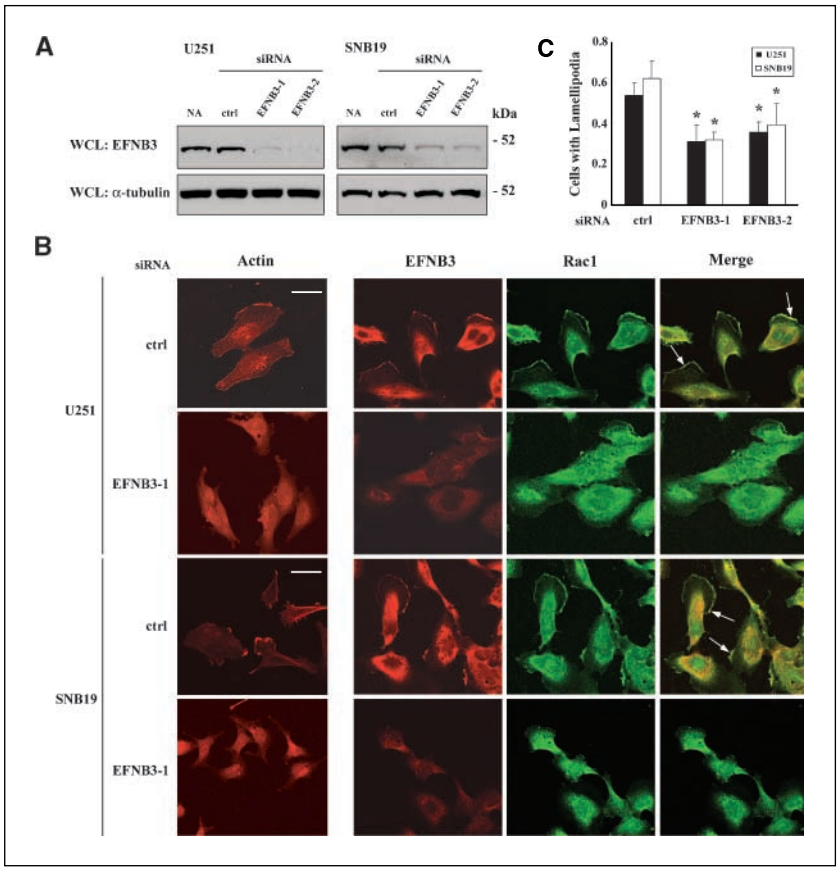

Figure 3. Morphologic change of U251 and SNB19 cells transfected with ephrin-B3 siRNA. *A,* Western blot showing reduction of ephrin-B3 protein expression following treatment with 20 nmol/L siRNA of either ephrin-B3-1 (*EFNB3-1*) or ephrin-B3-2 (*EFNB3-2*) in U251 and SNB19 cells. Nontransfected cells and luciferase siRNA serve as controls. *NA,* no addition. *WCL,* whole cell lysates. *B,* morphologic changes caused by depletion of ephrin-B3 and immunolocalization of ephrin-B3 and Rac1 in U251 and SNB19 cells. Cells were transfected with control luciferase (*ctrl*) or ephrin-B3-1 siRNA, and then stained for F-actin with Texas red–conjugated phalloidin and costained for ephrin-B3 (Cy3-stained) and Rac1 (FITC-stained). *Arrows,* colocalization of ephrin-B3 and Rac1 at lamellipodial formation. Bar, 50 μm. *C,* quantification of lamellipodial formation. *Columns,* percentage of transfected cells with lamellipodia covering at least quarter of the cell periphery in F-actin staining; *bars,* SD of four different measurements. At least 100 cells were counted for each determination. *, $P < 0.05$ versus control.

0.92 μm/h, $P < 0.05$, respectively) relative to mock-transfected cells (17.54 ± 2.05 and 11.24 ± 1.00 μm/h). The migration rate was enhanced by addition of EphB2/Fc chimera in the ephrin-B3 transfectants (27.04 ± 1.13 μm/h; $P < 0.01$; 14.83 ± 1.73 μm/h; $P < 0.05$; Fig. 2*B*), whereas no significant change was observed by adding control Fc to ephrin-B3 transfectants (data not shown).

As shown in Fig. 2*C*, cell invasion through membranes coated with Matrigel was increased in U87 and T98G cells expressing ephrin-B3 (mean ± SD, 146 ± 25% of mock control, $P < 0.05$; 132 ± 8% of mock control, $P < 0.05$, respectively) and in the cells treated with EphB2/Fc chimera (182 ± 16% of control, $P < 0.01$; 179 ± 11% of control, $P < 0.05$). As in the migration assays, no significant change was observed by adding control Fc to ephrin-B3 transfectants (data not shown). These data indicate that the activation of ephrin-B3 promotes glioma cell migration and invasion.

To evaluate effects of ephrin-B3 on invasion through a more physiologically relevant matrix, U87 and T98G cells cotransfected with GFP expression plasmids and control or ephrin-B3 vector were examined for their growth and dispersion within an *ex vivo* organotypic rat brain slice. Ephrin-B3 overexpressed in U87 and T98G cells was detected in the phosphorylated form, suggesting functional activation of ephrin-B3 (data not shown). To compare functional differences between mock and ephrin-B3 transfectants, aggregations of each transfected cell type were implanted in the putamen on contralateral sides of the same rat brain slice; images were taken at 12 and 48 hours after the implantation. The ephrin-B3-transfected cells displayed greater migration and invasion into the organotypic rat brain slice compared with the less invasive mock-transfectant cells (U87; Fig. 2*D*; T98G, data not shown). To quantify cell invasion, serial optical sections were obtained every 10 μm from the superior surface downward (*z*-axis) using confocal microscopy. The U87 and T98G-ephrin-B3 cells penetrated further into the brain slices (mean ± SD, 297.5 ± 38.6 μm/48 hours; 84.3 ± 13.2 μm/48 hours, respectively) than the mock cells (172.0 ± 18.4 μm/48 hours, $P < 0.05$; 49.7 ± 18.1 μm/48 hours, $P < 0.05$; Fig. 2*D*). Taken together, these data indicate that activation of ephrin-B3 accelerates glioma cell migration and invasion *in vitro* as well as *ex vivo*.

Depletion of ephrin-B3 decreases lamellipodial formation in glioma cells. To further examine functional effects of ephrin-B3, we used two different sequences of siRNA to specifically silent endogenous ephrin-B3 in high expressor U251 and SNB19 cells. Inhibition of ephrin-B3 mRNA was ~90% by both ephrin-B3-1 and ephrin-B3-2 siRNA and did not affect the expression levels of other ephrin-B family members (data not shown). Figure 3*A* confirms the reduction of ephrin-B3 protein expression in ephrin-B3-siRNA–transfected U251 and SNB19 cells compared with untransfected and luciferase siRNA controls.

Phalloidin staining for F-actin in U251 and SNB19 cells transfected with control siRNA was consistent with that normally seen in lamellipodia (Fig. 3*B*; ref. 35). Depletion of ephrin-B3 by transfection of ephrin-B3 siRNA interrupted lamellipodial formation in U251 and SNB19 (Fig. 3*C*), suggesting that ephrin-B3 plays a critical role in lamellipodia formation. Ephrin-B3 localized to the cell membrane in the control cells. Rac1, which regulates lamellipodial formation and cell migration, was also detected in the cytoplasm and on the cell surface, especially at leading membrane edges, as described previously (36, 37). Colocalization of ephrin-B3 with Rac1 was observed at the cell surface, suggesting a

significant interaction between ephrin-B3 and Rac1 (Fig. 3*B*). Cells transfected with siRNA for ephrin-B3 did not display any cytotoxic effects as determined by changes in 4′,6′-diamidino-2-phenylindole hydrochloride staining, propidium iodide uptake, and immunostaining with antiactivated caspase-3 antibodies (data not shown).

As expected, U87 and T98G cells overexpressing ephrin-B3 stimulated lamellipodial formation and ephrin-B3 colocalized with Rac1 (Supplementary Data 1), supporting our data that ephrin-B3 plays a role in lamellipodial formation through Rac1.

Depletion of ephrin-B3 decreases migration and invasion of glioma cells *in vivo* and *ex vivo*. To assess the phosphorylation level of ephrin-B3 in U251 and SNB19 cells transfected with control or ephrin-B3 siRNA, immunoprecipitation and Western blots were done. Endogenous phosphorylated ephrin-B3 was observed in both U251 and SNB19. Phosphorylation was enhanced by EphB2/Fc (Fig. 4*A*). Pretreatment with siRNA for ephrin-B3 reduced the phosphorylation level of ephrin-B3 concomitant with expression level.

Functional assays were done to confirm the effects of decreased phosphorylation of ephrin-B3 on migration of glioma cells. Ephrin-B2/Fc chimera stimulated migration of U251 and SNB19 glioma cells (9.36 ± 1.68 μm/h, $P < 0.05$; 16.40 ± 2.34 μm/h, $P < 0.01$, respectively) by ~1.31-fold and 1.42-fold, respectively, relative to cells treated with control siRNA (Fig. 4*B*). The migration of U251 and SNB19 was significantly suppressed by transfection of ephrin-B3-1 siRNA (5.09 ± 1.34 μm/h, $P < 0.05$; 6.99 ± 1.69 μm/h, $P < 0.01$) and ephrin-B3-2 siRNA (5.83 ± 1.04 μm/h, $P < 0.05$; 7.69 ± 1.32 μm/h, $P < 0.01$).

Invasion assay data also indicated that EphB2/Fc chimera stimulated invasion of U251 and SNB19 cells (138 ± 8% of control, $P < 0.01$; 187 ± 16% of control, $P < 0.01$, respectively; Fig. 4*C*). Two independent ephrin-B3 siRNAs inhibited the invasion of U251 and SNB19 cells (ephrin-B3-1, 57 ± 8% of control, $P < 0.01$; and 81 ± 8% of control, $P < 0.05$; ephrin-B3-2, 66 ± 12% of control, $P < 0.05$; and 88 ± 6% of control, $P < 0.05$, respectively) corresponding to the decreased expression of ephrin-B3. Furthermore, depletion of endogenous ephrin-B3 expression by ephrin-B3 siRNA transfection abrogated the increase of migration and invasion by EphB2/Fc stimuli in U251 and SNB19 cells (Fig. 4*B* and *C*), indicating that the increased migration and invasion is dependent on ephrin-B3 activation.

In addition, *ex vivo* organotypic rat brain slice invasion assays showed that U251- and SNB19-ephrin-B3 siRNA-transfected cells

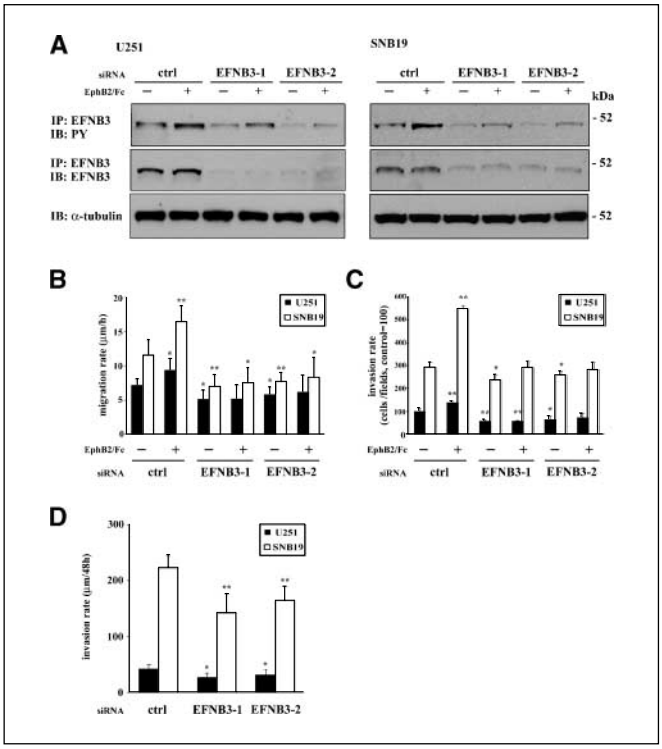

Figure 4. Suppression of migration and invasion by ephrin-B3 siRNA in U251 and SNB19 cells. *A,* extracts of cells transfected with luciferase (control) or ephrin-B3 siRNA were immunoprecipitated (*IP*) with anti-ephrin-B3 antibody. Cells were treated with 1.0 μg/mL soluble EphB2/Fc chimera or control Fc for 10 minutes before collection. The immunoprecipitates were probed by immunoblotting (*IB*) as indicated. Whole cell lysates were also immunoblotted with anti-α-tubulin antibody as a loading control. *PY,* phosphotyrosine. *B,* cells were plated onto 10-well glass slides precoated with astrocytoma-derived extracellular matrix, and then cultured in serum-free medium in the absence or presence of 1.0 μg/mL soluble EphB2/Fc after the attachment of the cells to the dishes. *Columns,* cell migration rate assessed over 24 hours; *bars,* SE. *, $P < 0.05$; **, $P < 0.01$ versus control without EphB2/Fc stimuli. *C,* cells were treated as above, then applied to the invasion assay. *Columns,* mean cell counts from at least six fields and four experiments; *bars,* SE. *, $P < 0.05$; **, $P < 0.01$ versus control without EphB2/Fc stimuli. *D,* invasion rates (*columns*) of U251 and SNB19 cells stably expressing GFP and transfected with ephrin-B3 siRNA or control siRNA were calculated as in Fig. 2*E*; *bars,* SE. *, $P < 0.05$; **, $P < 0.01$ versus control.

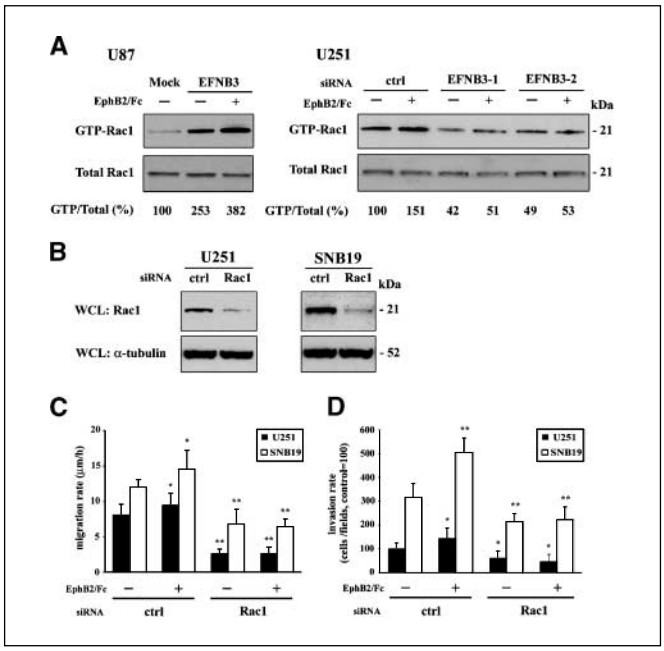

Figure 5. Ephrin-B3 is associated with Rac1 activation. *A,* U87 cells transfected with pEAK (mock) or ephrin-B3 and treated with 1.0 μg/mL soluble EphB2/Fc chimera or control Fc for 10 minutes were subjected to a Rac1 pull-down assay. Extracts of U251 cells transfected with luciferase (control) or ephrin-B3 siRNA were also subjected to a Rac1 pull-down assay. The numerical values indicate relative ratios as a percentage of the control for each band of GTP-Rac1/total-Rac1 after scanning and densitometric analysis using software by NucleoVision (NucleoTech, San Mateo, CA). *B,* Western blot showing reduction of Rac1 protein expression following treatment with 20 nmol/L Rac1 siRNA in U251 and SNB19 cells. Luciferase siRNA served as a control. *C,* cells treated with siRNA were plated onto 10-well glass slides precoated with astrocytoma-derived extracellular matrix, and then cultured in serum-free medium in the absence or presence of 1.0 μg/mL soluble EphB2/Fc after the attachment of the cells to the dishes. *Columns,* cell migration assessed over 24 hours; *bars*, SE. *, $P < 0.05$; **, $P < 0.01$ versus control without EphB2/Fc stimuli. *D,* cells were treated as above, then applied to the invasion assay. *Columns,* mean cell counts from at least six fields in each of four experiments; *bars*, SE. *, $P < 0.05$; **, $P < 0.01$ versus control without EphB2/Fc stimuli.

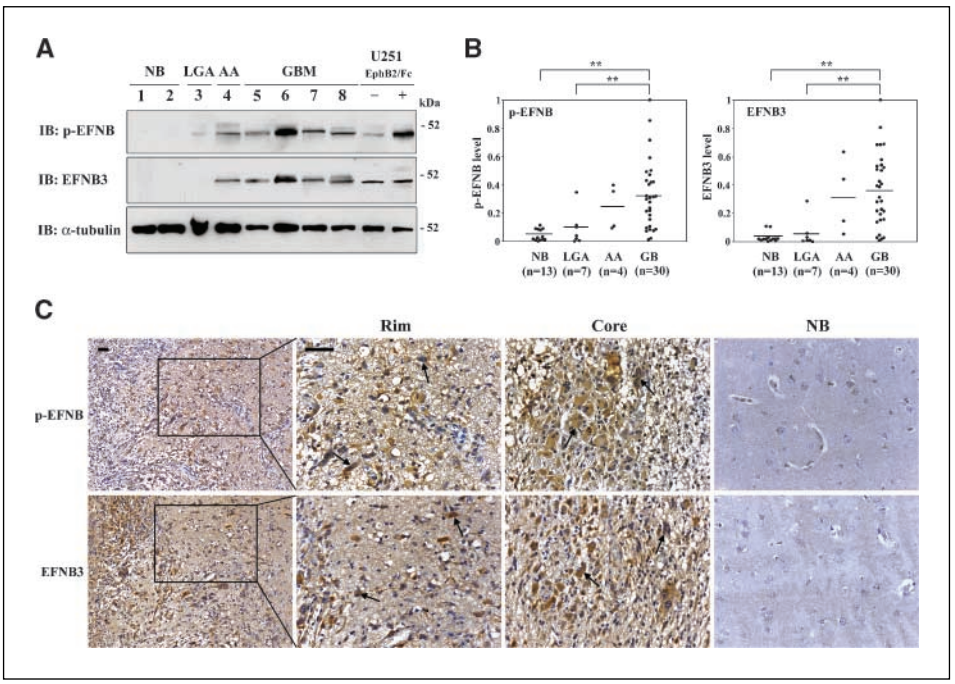

Figure 6. Ephrin-B3 expression, phosphorylation, and localization in various human astrocytic tumors. *A,* the total cell lysate from normal brains (*lanes 1 and 2, NB*), low-grade astrocytomas (*lane 3, LGA*), anaplastic astrocytomas (*lane 4, AA*), glioblastomas (*lanes 5-8, GBM*), and U251 cells treated with or without EphB2/Fc (*lanes 9 and 10*) were subjected to Western blotting. Eight representative samples. Equal amounts of cell lysates were immunoblotted with antiphosphorylated ephrin-B (*p-EFNB*) antibody. The membrane was stripped and reprobed with anti-ephrin-B3 (*EFNB3*) and anti-α-tubulin antibodies. *B,* signals were quantified by densitometry using Gel Expert software by Nucleovision. Relative protein expression levels of phosphorylated ephrin-B (phosphorylated ephrin-B protein/α-tubulin protein ratios) and ephrin-B3 (ephrin-B3 protein/α-tubulin protein ratios) in tumor tissues and normal brain were determined. Each protein level is expressed as a proportion of the highest protein level of phosphorylated ephrin-B or ephrin-B3, which was given a value of 1. *Horizontal bars,* mean values. **, $P < 0.01$. *C,* immunolocalization of phosphorylated ephrin-B and ephrin-B3 in glioblastoma tissues and normal brain tissues. Paraffin sections were immunostained with antibodies against phosphorylated ephrin-B or ephrin-B3. Note that phosphorylated ephrin-B and ephrin-B3 are immunolocalized in the glioblastoma cells at the central region of the tumor (*Core*), as well as in invading glioblastoma cells at the tumor border (*Rim*), whereas no staining is observed in the normal brain. Hematoxylin counterstain. Bar, 50 μm.

penetrated into the brain slices less (ephrin-B3-1, 27.5 ± 7.6 μm/48 hours and 141.5 ± 34.9 μm/48 hours; ephrin-B3-2, 31.0 ± 10.2 μm/48 hours and 164.0 ± 24.0 μm/48 hours, respectively) than the control cells (42.5 ± 7.0 μm/48 hours, $P < 0.05$; 221.5 ± 23.6 μm/48 hours, $P < 0.01$; Fig. 4*D*). These data suggest that ephrin-B3 plays a role in invasion both *in vitro* and *ex vivo*.

Ephrin-B3 is associated with Rac1 activation. The observation that ephrin-B3 was involved in lamellipodial formation, and that ephrin-B3 colocalized with Rac1, suggested that Rac1 activation was a possible mechanism involved in ephrin-B3-related motility of glioma cells. To confirm this, we used Rac1-GTP pull-down assays on lysates from U87 and U251 cells. Rac1 activation was promoted by transfecting U87 cells with ephrin-B3 (2.5-fold). This activation was further prompted by addition of EphB2/Fc (Fig. 5*A*). Moreover, U251 cells treated with two independent siRNAs for ephrin-B3 showed decreased Rac1 activity compared with control siRNA-transfected cells (0.4- to 0.5-fold; Fig. 5*A*). Addition of EphB2/Fc promoted Rac1 activation in U251 cells transfected with control siRNA (1.5-fold). Incomplete depletion of ephrin-B3 may be attributable to slight enhanced activation of Rac1 by EphB2/Fc in ephrin-B3 knockdown cells. These data suggest that Rac1 activation is associated with phosphorylation of ephrin-B3.

To further examine the role of Rac1 downstream of ephrin-B3 in glioma cells, we did Rac1-directed siRNA experiments. Figure 5*B* confirms the reduction of Rac1 protein expression in Rac1-siRNA-treated U251 and SNB19 cells compared with luciferase siRNA controls. Cells transfected with luciferase or Rac1 siRNA were placed in the radial cell migration assay. Rac1 depletion inhibited the migration of U251 and SNB19 cells by ~0.3-fold and 0.5-fold, respectively (Fig. 5*C*). Moreover, Rac1-directed siRNA treatment effectively abrogated the EphB2/Fc-induced motility of U251 and SNB19 cells (Fig. 5*C*).

As shown in Fig. 5*D*, similar findings were obtained with invasion assays. Cell invasion through Matrigel-coated membranes decreased in cells transfected with Rac1 siRNA by ~0.6-fold in U251 and 0.7-fold in SNB19, compared with cells transfected with control siRNA. The EphB2/Fc-induced motility of U251 and SNB19 cells was effectively counteracted by Rac1-directed siRNA treatment. Taken together, these data indicate that ephrin-B3 is strongly associated with Rac1 activation and this interaction is critical to glioma cell migration and invasion.

Overexpression and phosphorylation of ephrin-B3 in glioblastoma. To evaluate a potential role for ephrin-B3 in the malignant behavior of human gliomas, immunoblotting by a specific antibody against phosphorylated ephrin-B was done using 54 surgical specimens, as well as U251 cells treated with or without EphB2/Fc as a control. Phosphorylated ephrin-B was detected in anaplastic astrocytomas and glioblastomas, but not in the normal brain (Fig. 6*A*). Signals were quantified by densitometry and levels of phosphorylated ephrin-B were evaluated using α-tubulin as an internal control for normalization (phosphorylated ephrin-B/α-tubulin protein ratios). Phosphorylated ephrin-B increased as a function of tumor grade (normal brain, 0.04 ± 0.04, $n = 13$; low-grade astrocytoma, 0.09 ± 0.12, $n = 7$; anaplastic astrocytoma,

0.24 ± 0.16, n = 4; glioblastoma, 0.32 ± 0.24, n = 30; Fig. 6*B*). The membranes were stripped and an ephrin-B3 antibody was applied. The band of ephrin-B3 was identical to phosphorylated ephrin-B at 50 kDa (Fig. 6*A*) and protein levels of ephrin-B3 were significantly higher in glioblastoma tissues (0.36 ± 0.26, $P < 0.01$) relative to normal brain tissues (0.03 ± 0.04) and low-grade astrocytoma tissues (0.06 ± 0.10; Fig. 6*B*). In addition, the level of phosphorylated ephrin-B directly correlated with the level of total ephrin-B3 in each glioblastoma case (n = 30, r = 0.843, $P < 0.01$, data not shown). Furthermore, the band was recognized at a similar level in U251, which is a high expressor of ephrin-B3 but low expressor of ephrin-B1 and ephrin-B2 (Fig. 1*A*). These data suggest that phosphorylated ephrin-B was highly expressed in malignant astrocytomas and that the phosphorylated ephrin-B is most likely the ephrin-B3 isoform.

Cells expressing phosphorylated ephrin-B and ephrin-B3 in normal brain and glioblastoma specimens were identified using immunohistochemistry. Tyrosine-phosphorylated ephrin-B and ephrin-B3 were immunolocalized predominantly to the majority of neoplastic astrocytes in all of the glioblastoma specimens (15 of 15 cases; Fig. 6*C*). Invading neoplastic cells also showed significant staining for phosphorylated ephrin-B and ephrin-B3. Neoplastic astrocytes were identified by nuclear atypia in H&E-stained sections and were confirmed by immunopositivity for glial fibrillary acidic protein staining (data not shown). Endothelial cells of blood vessels in the glioblastoma tissues and reactive astrocytes occasionally immunostained for phosphorylated ephrin-B and ephrin-B3. No staining was observed in normal brain (Fig. 6*C*) or when the primary antibody was substituted for normal serum (data not shown). The immunohistochemistry results were consistent with that of the immunoblot analysis.

Discussion

Eph receptors and their ligands are important in regulating cell-cell interactions by initiating unique bidirectional signal transduction. Evidence presented here verifies the effect of ephrin-B3 on glioma cell motility *in vitro* and *in vivo*. Actively migrating cells displayed greater expression of ephrin-B3 in four of four glioma cell lines. Forced expression of ephrin-B3 in U87 and T98G, which have low constitutive expression of ephrin-B3, transformed the cells into a more highly invasive phenotype. Depletion of ephrin-B3 by siRNA treatment in U251 and SNB19, which are high expressors of ephrin-B3, decreased migration and invasion. Ephrin-B3 was localized to the leading edge at sites of lamellipodial formation in U251 and SNB19. The small GTPase Rac1 was activated by forced expression of ephrin-B3 in U87 and deactivated by siRNA for ephrin-B3 in U251. Additionally, the depletion of ephrin-B3 and Rac1 abrogated the increase of migration and invasion by EphB2/Fc in U251 and SNB19, suggesting that this increase is dependent on ephrin-B3/Rac1 signaling. The expression and phosphorylation of ephrin-B3 were up-regulated in glioblastoma specimens, especially in invading cells. These results strongly implicate ephrin-B3/Rac1 signaling in glioblastoma invasion.

Ephrin-B3 shares 48.8% and 49.3% amino acid homology with ephrin-B1 and ephrin-B2, respectively, but the homology between human and mouse ephrin-B3 is >96% (38). This high degree of homology suggests an important conserved function of ephrin-B3. Ephrin-B3 has been noted for its remarkably restricted expression pattern down the midline of the neural tube during development (8, 38), suggesting that ephrin-B3 may regulate the midline guidance of axons in forming the spinal cord. In addition, it has also been reported that ephrin-B3 guides regional innervation by suppressing axonal growth of lateral thalamic neurons in developing rat brains (39). Thus, ephrin-B3 is likely to play a critical role in the process of neurodevelopment. Recent studies reported that ephrin-B3 expressed in myelinating oligodendrocytes in the adult mouse spinal cord inhibits regeneration of the central nervous system after injury by interrupting neurite outgrowth (40). This indicates that ephrin-B3 is involved in pathologic conditions of the central nervous system. Ephrin-B3 expression has been verified in both fetal brain and adult brain (41). However, our data shows that phosphorylated ephrin-B3 is below detection levels in normal brain, suggesting that ephrin-B3 signaling may not affect normal physiologic processes of the adult brain.

Accumulating evidence indicates that high expression of ephrins may be associated with increased potential for tumor growth, tumorigenicity, and metastasis (15, 42). Currently, no data have been reported concerning the induction of cell motility by ephrin-B3, although it is well established that ephrin-B1 and ephrin-B2 mediate cell migration (43–46). Ephrin-B expression has been reported in various human cancers, including carcinomas of the lung (14) and colon (47), as well as melanoma (15) and neuroblastoma (48). Ephrin-B3 expression in particular was confirmed in small-cell lung carcinoma (14) and neuroblastoma (48). However, its role in invasion and metastasis in human carcinomas has not been previously described. The data in the present study show a strong correlation between the phosphorylation level of ephrin-B3 and glioma migration and invasion rates. Thus, this study is the first to reveal that the kinase activity of the ephrin-B3 ligand is involved in tumor invasion activity and possibly malignant progression in human tumors.

Based on our recent description of the overexpression of EphB2 in glioblastoma (21), an engineered soluble receptor EphB2/Fc chimera was used for stimulation of ephrin-B3. As expected, endogenous ephrin-B3 was phosphorylated by EphB2/Fc in U251 and SNB19, and exogenous ephrin-B3 was also phosphorylated in U87 and T98G. Our results are consistent with previous findings that Fc fusions of EphB2 bind to ephrin-B3 (49). In addition, our data show that the reverse signaling stimulated by EphB2 is dependent on ephrin-B3 in U251 and SNB19 cells. Thus, the expression of EphB2 and ephrin-B3 in human glioma cell lines and tumor surgical specimens supports the possibility of autocrine or paracrine loops mediated by EphB2 receptor and ephrin-B3 ligand in human gliomas. Additional autocrine loops mediated by other EphB receptor family members and ephrin-B ligands may operate in human gliomas. In fact, our preliminary data showed that EphB4, ephrin-B1, and ephrin-B2 transcripts were expressed in several glioma cell lines and glioma surgical specimens, and have some effect on invasion (data not shown). Additional analysis of the expression and function of other EphB receptor kinases and ephrin-B ligands will be required to further address this question.

The activated form of Rac1 is well known to stimulate cell migration through actin reorganization and formation of lamellipodia (36, 37). We showed that U251 and SNB19 cells transfected with ephrin-B3 siRNA manifest dramatic morphologic changes, decreased lamellipodial formation, and suppressed migration and invasion activity. In contrast, U87 and T98G cells transfected with ephrin-B3 increased lamellipodial formation and promoted migration and invasion. As expected from these phenotypic changes and colocalization of ephrin-B3 with Rac1, Rac1 was deactivated by the silencing of ephrin-B3 using siRNA in U251, whereas forced

expression of ephrin-B3 in U87 activated Rac1. This is somewhat anticipated, because the tyrosine phosphorylated motifs of ephrin-B can associate with Rac through the SH2/SH3 adaptor Grb4, which may recruit a Rac exchange factor to the ephrin-B (50). In addition, our data show that depletion of Rac1 abrogates the effect of ephrin-B3 signaling stimulated by EphB2/Fc, indicating ephrin-B3 signaling is dependent on Rac1. Recent investigations, including ours, revealed that Rac1 plays a major role in glioma invasion (25, 26, 34). Thus, these data suggest that ephrin-B3 mediates morphologic changes and promotes migration and invasion through Rac1 activation. Similar findings have been shown with the ephrin-B1 ligand, which was revealed to activate Rac1 through Tiam1, a specific guanine-nucleotide exchange factor for Rac1 (24). We observed in preliminary investigations that ephrin-B3 does not interact with Rac1 directly, as assessed by immunoprecipitation (data not shown). We speculate that ephrin-B3 activates Rac1 in a manner similar to ephrin-B1. Further investigation into the activation mechanism of Rac1 by ephrin-B3 is under way in our laboratory.

Lastly, the evidence presented here show that the level of tyrosine phosphorylated ephrin-B protein is significantly higher in glioblastoma tissue than in normal brain or low-grade astrocytoma, and that the phosphorylated ephrin-B is likely derived from ephrin-B3, suggesting a high level of phosphorylated ephrin-B3 in glioblastoma. Additionally, because phosphorylated ephrin-B and ephrin-B3 protein immunolocalized predominantly to glioma cells, the increase of phosphorylated ephrin-B3 protein in glioblastoma tissue is ascribed to astrocytic tumor cells. Thus, confirmation of phosphorylated ephrin-B and ephrin-B3 production in invading glioblastoma cells by immunohistochemistry, along with QRT-PCR data verifying the overexpression of ephrin-B3 in these cells, suggests that the production level of ephrin-B3 is up-regulated and phosphorylated in invading cells. Together, the *in vitro* and *in vivo* data indicate that the up-regulation and phosphorylation of ephrin-B3 in glioma tissues contributes to the malignant behavior of glioblastoma and may drive invasion of glioma cells into normal brain tissue.

In conclusion, this study reveals the biological significance of ephrin-B3 expression in glioma and illustrates that phosphorylation of ephrin-B3 is associated with heightened invasive activity of glioma cells. Phenotypic consequences of activated ephrin-B3 are dependent on the activation of Rac1. Our discovery of the involvement of ephrin-B3/Rac1 in glioma invasion provides insight into this signaling pathway as a potential therapeutic target, and proposes a new paradigm of promoting glioma invasion through specific cell-cell interactions.

Acknowledgments

Received 11/28/2005; revised 5/22/2006; accepted 6/23/2006.

Grant support: NIH grant NS042262 (M.E. Berens) and Fellowship Award for Research Abroad from Japan Society for the Promotion of Science (M. Nakada).

The costs of publication of this article were defrayed in part by the payment of page charges. This article must therefore be hereby marked *advertisement* in accordance with 18 U.S.C. Section 1734 solely to indicate this fact.

We thank Drs. Hiroshi Sato and Hisashi Miyamori for making expression vector; Dominique B. Hoelzinger, Wendy S. McDonough, Christian E. Beaudry, Kirsten A. Vryhof, and Joshua R. Niska for technical assistance; Dr. Spyro Mousses and Don Weaver for designing siRNA for ephrin-B3; Dr. Jie Wu for assisting in organotypic brain slice culture; and Dr. Nhan L. Tran, Dr. Tim Demuth, Dr. Anna M. Joy, Dr. Marc Symons, and Jessica L. Rennert for their valuable discussion.

References

1. Lemke G. A coherent nomenclature for Eph receptors and their ligands. Mol Cell Neurosci 1997;9:331–2.
2. Pasquale EB. Eph receptor signalling casts a wide net on cell behaviour. Nat Rev Mol Cell Biol 2005;6:462–75.
3. Kullander K, Klein R. Mechanisms and functions of Eph and ephrin signalling. Nat Rev Mol Cell Biol 2002;3:475–86.
4. Klein R. Excitatory Eph receptors and adhesive ephrin ligands. Curr Opin Cell Biol 2001;13:196–203.
5. Wilkinson DG. Multiple roles of EPH receptors and ephrins in neural development. Nat Rev Neurosci 2001;2:155–64.
6. Mellitzer G, Xu Q, Wilkinson DG. Control of cell behaviour by signalling through Eph receptors and ephrins. Curr Opin Neurobiol 2000;10:400–8.
7. Dodelet VC, Pasquale EB. Eph receptors and ephrin ligands: embryogenesis to tumorigenesis. Oncogene 2000;19:5614–9.
8. Gale NW, Holland SJ, Valenzuela DM, et al. Eph receptors and ligands comprise two major specificity subclasses and are reciprocally compartmentalized during embryogenesis. Neuron 1996;17:9–19.
9. Zimmer M, Palmer A, Kohler J, Klein R. EphB-ephrinB bi-directional endocytosis terminates adhesion allowing contact mediated repulsion. Nat Cell Biol 2003;5:869–78.
10. Marston DJ, Dickinson S, Nobes CD. Rac-dependent *trans*-endocytosis of ephrinBs regulates Eph-ephrin contact repulsion. Nat Cell Biol 2003;5:879–88.
11. Irie F, Okuno M, Pasquale EB, Yamaguchi Y. EphrinB-EphB signalling regulates clathrin-mediated endocytosis through tyrosine phosphorylation of synaptojanin 1. Nat Cell Biol 2005;7:501–9.
12. Cheng N, Brantley DM, Chen J. The ephrins and Eph receptors in angiogenesis. Cytokine Growth Factor Rev 2002;13:75–85.
13. Surawska H, Ma PC, Salgia R. The role of ephrins and Eph receptors in cancer. Cytokine Growth Factor Rev 2004;15:419–33.
14. Tang XX, Brodeur GM, Campling BG, Ikegaki N. Coexpression of transcripts encoding EPHB receptor protein tyrosine kinases and their ephrin-B ligands in human small cell lung carcinoma. Clin Cancer Res 1999;5:455–60.
15. Vogt T, Stolz W, Welsh J, et al. Overexpression of Lerk-5/Eplg5 messenger RNA: a novel marker for increased tumorigenicity and metastatic potential in human malignant melanomas. Clin Cancer Res 1998;4:791–7.
16. Mao W, Luis E, Ross S, et al. EphB2 as a therapeutic antibody drug target for the treatment of colorectal cancer. Cancer Res 2004;64:781–8.
17. Wu Q, Suo Z, Risberg B, Karlsson MG, Villman K, Nesland JM. Expression of Ephb2 and Ephb4 in breast carcinoma. Pathol Oncol Res 2004;10:26–33.
18. Lugli A, Spichtin H, Maurer R, et al. EphB2 expression across 138 human tumor types in a tissue microarray: high levels of expression in gastrointestinal cancers. Clin Cancer Res 2005;11:6450–8.
19. Hatano M, Eguchi J, Tatsumi T, et al. EphA2 as a glioma-associated antigen: a novel target for glioma vaccines. Neoplasia 2005;7:717–22.
20. Wykosky J, Gibo DM, Stanton C, Debinski W. EphA2 as a novel molecular marker and target in glioblastoma multiforme. Mol Cancer Res 2005;3:541–51.
21. Nakada M, Niska JA, Miyamori H, et al. The phosphorylation of EphB2 receptor regulates migration and invasion of human glioma cells. Cancer Res 2004;64:3179–85.
22. Hoelzinger DB, Mariani L, Weis J, et al. Gene expression profile of glioblastoma multiforme invasive phenotype points to new therapeutic targets. Neoplasia 2005;7:7–16.
23. Nakada M, Niska JA, Tran NL, McDonough WS, Berens ME. EphB2/R-Ras signaling regulates glioma cell adhesion, growth, and invasion. Am J Pathol 2005;167:565–76.
24. Tanaka M, Ohashi R, Nakamura R, et al. Tiam1 mediates neurite outgrowth induced by ephrin-B1 and EphA2. EMBO J 2004;23:1075–88.
25. Murai T, Miyazaki Y, Nishinakamura H, et al. Engagement of CD44 promotes Rac activation and CD44 cleavage during tumor cell migration. J Biol Chem 2004;279:4541–50.
26. Chuang YY, Tran NL, Rusk N, Nakada M, Berens ME, Symons M. Role of synaptojanin 2 in glioma cell migration and invasion. Cancer Res 2004;64:8271–5.
27. Giese A, Rief MD, Loo MA, Berens ME. Determinants of human astrocytoma migration. Cancer Res 1994;54:3897–904.
28. Berens ME, Rief MD, Loo MA, Giese A. The role of extracellular matrix in human astrocytoma migration and proliferation studied in a microliter scale assay. Clin Exp Metastasis 1994;12:405–15.
29. Kleihues P, Louis DN, Scheithauer BW, et al. The WHO classification of tumors of the nervous system. J Neuropathol Exp Neurol 2002;61:215–25; discussion 226–9.
30. Mariani L, McDonough WS, Hoelzinger DB, et al. Identification and validation of P311 as a glioblastoma invasion gene using laser capture microdissection. Cancer Res 2001;61:4190–6.
31. Takino T, Nakada M, Miyamori H, Yamashita J, Yamada KM, Sato H. CrkI adapter protein modulates cell migration and invasion in glioblastoma. Cancer Res 2003;63:2335–7.
32. Nakada M, Miyamori H, Kita D, et al. Human glioblastomas overexpress ADAMTS-5 that degrades brevican. Acta Neuropathol (Berl) 2005;110:239–46.
33. Valster A, Tran NL, Nakada M, Berens ME, Chan AY, Symons M. Cell migration and invasion assays. Methods 2005;37:208–15.
34. Salhia B, Rutten F, Nakada M, et al. Inhibition of Rho-kinase affects astrocytoma morphology, motility, and

invasion through activation of Rac1. Cancer Res 2005;65:8792–800.
35. Small JV, Stradal T, Vignal E, Rottner K. The lamellipodium: where motility begins. Trends Cell Biol 2002;12:112–20.
36. Nobes CD, Hall A. Rho, rac, and cdc42 GTPases regulate the assembly of multimolecular focal complexes associated with actin stress fibers, lamellipodia, and filopodia. Cell 1995;81:53–62.
37. Fukata M, Nakagawa M, Kaibuchi K. Roles of Rho-family GTPases in cell polarisation and directional migration. Curr Opin Cell Biol 2003;15:590–7.
38. Bergemann AD, Zhang L, Chiang MK, Brambilla R, Klein R, Flanagan JG. Ephrin-B3, a ligand for the receptor EphB3, expressed at the midline of the developing neural tube. Oncogene 1998;16:471–80.
39. Takemoto M, Fukuda T, Sonoda R, Murakami F, Tanaka H, Yamamoto N. Ephrin-B3-4 interactions regulate the growth of specific thalamocortical axon populations *in vitro*. Eur J Neurosci 2002;16:1168–72.
40. Benson MD, Romero MI, Lush ME, Lu QR, Henkemeyer M, Parada LF. Ephrin-B3 is a myelin-based inhibitor of neurite outgrowth. Proc Natl Acad Sci U S A 2005;102:10694–9.
41. Tang XX, Pleasure DE, Ikegaki N. cDNA cloning, chromosomal localization, and expression pattern of EPLG8, a new member of the EPLG gene family encoding ligands of EPH-related protein-tyrosine kinase receptors. Genomics 1997;41:17–24.
42. Easty DJ, Hill SP, Hsu MY, et al. Up-regulation of ephrin-A1 during melanoma progression. Int J Cancer 1999;84:494–501.
43. Huynh-Do U, Vindis C, Liu H, et al. Ephrin-B1 transduces signals to activate integrin-mediated migration, attachment and angiogenesis. J Cell Sci 2002;115:3073–81.
44. Steinle JJ, Meininger CJ, Chowdhury U, Wu G, Granger HJ. Role of ephrin B2 in human retinal endothelial cell proliferation and migration. Cell Signal 2003;15:1011–7.
45. Noren NK, Lu M, Freeman AL, Koolpe M, Pasquale EB. Interplay between EphB4 on tumor cells and vascular ephrin-B2 regulates tumor growth. Proc Natl Acad Sci U S A 2004;101:5583–8.
46. Meyer S, Hafner C, Guba M, et al. Ephrin-B2 overexpression enhances integrin-mediated ECM-attachment and migration of B16 melanoma cells. Int J Oncol 2005;27:1197–206.
47. Liu W, Ahmad SA, Jung YD, et al. Coexpression of ephrin-Bs and their receptors in colon carcinoma. Cancer 2002;94:934–9.
48. Tang XX, Evans AE, Zhao H, et al. High-level expression of EPHB6, EFNB2, and EFNB3 is associated with low tumor stage and high TrkA expression in human neuroblastomas. Clin Cancer Res 1999;5:1491–6.
49. Gale NW, Flenniken A, Compton DC, et al. Elk-L3, a novel transmembrane ligand for the Eph family of receptor tyrosine kinases, expressed in embryonic floor plate, roof plate and hindbrain segments. Oncogene 1996;13:1343–52.
50. Noren NK, Pasquale EB. Eph receptor-ephrin bidirectional signals that target Ras and Rho proteins. Cell Signal 2004;16:655–66.

Ephrin-B3 Ligand Promotes Glioma Invasion through Activation of Rac1

Mitsutoshi Nakada, Kelsey L. Drake, Satoko Nakada, et al.

Cancer Res 2006;66:8492-8500.